JOURNAL OF COMPUTATIONAL PHYSICS 68, 393–419 (1987)

Hybrid Approximate Solution–Approximate Potential Approach to the Solution of Coupled Equations for Atom–Molecule Reactive Scattering

FELICJA MRUGAŁA

Institute of Physics, Nicholas Copernicus University, Toruń, Poland

Received February 5, 1985; revised April 30, 1986

The generalized log-derivative method is applied to the coupled equations problem for collinear atom–molecule reactions formulated in terms of natural collision coordinates. A comparison with the "$\mathscr{R}$-matrix propagation" method is made. The comparison is based on numerical tests performed on the $H+H_2$ reaction. Some tests were made also on the asymmetric $F+H_2$ system. In consequence of these tests two hybrid versions of the *RXN1D* program were developed. They are demonstrated to be about two times faster than the original version.

1. INTRODUCTION

The purposefulness of hybridizing the approximate solution and the approximate potential approaches within the invariant embedding technique [1] as a methodology of deriving efficient algorithms for solving the coupled equations of molecular scattering theory seems to be unquestionable. The VIVAS program [2, 3] has been developed in this way, and in the 1981 comparative study on numerical methods [4] it was found to be the most efficient program available for solving inelastic scattering problems. Despite the encouraging success of this program, however, to our knowledge, not much has been done since then to take advantage of the high efficiency of hybrid methods in other fields of scattering calculations. Believing that this situations should be improved we have undertaken the investigations directed toward extending the use of hybrid methods to reactive scattering problems.

Judging by the numerous quotations in the present-day literature, one of the best computational techniques devised for treating atom-molecule reactive systems is the "$\mathscr{R}$-matrix propagation" method [6, 7, 8] coded in the *RXN1D* program [5]. This is a purely approximate potential-type method, however. So, a considerable improvement in efficiency could be expected if this method were properly combined with an approximate solution-type method of comparable quality. Two such

0021-9991/87 $3.00

581/68/2-10

methods have become available recently. These are the "$\mathscr{L}$-matrix" methods [11, 12] derived as generalizations of the log-derivative method of Johnson [9, 10] and designed to solve the coupled equations problems formulated in the diabatic and in the nondiabatic representations, respectively.

Both "$\mathscr{L}$-matrix" methods are adapted in Section 3 of this paper to the description of collinear $AB+C \rightleftarrows A+BC$ reactions outlined in Section 2. In Section 4 they are tested against the "$\mathscr{R}$-matrix propagation" method on the case of the $H+H_2$ reaction and, to a lesser extent, on the asymmetric $F+H_2$ reactive system. All tests presented were performed with the use of properly modified versions of the *RXN1D* program. Much attention is paid to the construction of hybrid versions of this program and we demonstrate their superiority to the original version.

2. The Collinear $A+BC \rightleftarrows AB+C$ Reactive Scattering Problem

To fix the terminology we start with a skechy description of the coordinate system which is used here as originally devised by Light *et al.* [6, 13]. The reaction coordinate, u, is defined as an arc length along a specified reference curve (RC) and the vibrational coordinate, v, is measured along straight lines locally orthogonal to this curve. The reference curve is set on a given potential surface for the *A-B-C* system in a way basically consistent with the idea of a natural coordinate system [14, 15].

The characteristic features of this particular system are

(1) the discontinuity of RC at its crossing with the line dividing the configuration space into the arrangements channels: the channel α containing the asymptotic $A+BC$ configuration and the channel γ containing the $AB+C$ configuration,

(2) the subdivision of each arrangement channel into two regions: the polar region (P) where the (RC) has nonzero constant curvature; $1/\sigma$, and the Cartesian region (C) where RC becomes a straight line.

The wavefunction expressed in the (u, v) coordinates satisfies the Schrödinger equation of the form:

$$\left[-\frac{\hbar^2}{2\mu}\left(\frac{1}{\eta^2}\frac{\partial^2}{\partial u^2}+\frac{1}{\eta}\frac{\partial}{\partial v}\eta\frac{\partial}{\partial v}\right)+V(u,v)\right]\Psi(u,v)=E\Psi(u,v)$$

and the following continuity conditions which should be imposed at the polar-Cartesian boundary in each arrangement channel, where $u_a=u_a^{P-C}$ for $a=\alpha, \gamma$;

$$\Psi^P=\Psi^C, \qquad \frac{1}{\eta^P}\frac{\partial\Psi^P}{\partial u_a}=\frac{1}{\eta^c}\frac{\partial\Psi^c}{\partial u_a},$$

and at the common channel boundary where $u_a = 0$ for $a = \alpha, \gamma$;

$$\Psi^\alpha = \Psi^\gamma, \qquad -\frac{1}{\eta_\alpha}\frac{\partial \Psi^\alpha}{\partial u_\alpha} = \frac{1}{\eta_\gamma}\frac{\partial \Psi^\gamma}{\partial u_\gamma},$$

μ, V, E denote the reduced mass of the A-B-C system, the potential and the total energy, respectively. η is the Jacobian of the transformation from the mass-weighted Cartesian to the (u, v) coordinates. It equals $1 + (v/\sigma)$ in the polar and 1 in the Cartesian region of the u-coordinate [6]. Now, applying the factorization [20];

$$\Psi(u, v) = \eta^{1/2}\psi(u, v),$$

and expanding the function $\psi(u, v)$ in an appropriate basis of vibrational functions,

$$(\phi_1(v; u), \phi_2(v; u), \ldots, \phi_N(v; u)) = \Phi^T(v; u),$$

which change along the reaction coordinate continuously (within one region at least);

$$\psi(u, v) = \Phi^T(v; u) f(u),$$

we can formulate the problem in terms of the following coupled equations;

$$\left[\frac{d^2}{du^2} + A(u)\frac{d}{du} + B(u)\right] f(u) = 0 \tag{3}$$

and the following conditions for matching solutions of these equations, and their derivatives, i.e., the vectors

$$\begin{pmatrix} f(u) \\ \dfrac{d}{du} f(u) \end{pmatrix} = \mathscr{F}(u), \tag{3a}$$

at the P-C and at the α-γ boundaries

$$\mathscr{S}^P(u^{P-C})\,\mathscr{F}^P(u^{P-C}) = \mathscr{T}^{P-C}\mathscr{S}^C(u^{P-C})\,\mathscr{F}^C(u^{P-C}), \tag{4a}$$

$$\mathscr{S}^\alpha(u_\alpha = 0)\,\mathscr{F}^\alpha(u_\alpha = 0) = I_-\,\mathscr{T}^{\alpha-\gamma}\mathscr{S}^\gamma(u_\gamma = 0)\,\mathscr{F}^\gamma(u_\gamma = 0), \tag{4b}$$

where

$$\mathscr{T}^{P-C} = \begin{pmatrix} C_1 & 0 \\ 0 & C_2 \end{pmatrix}, \qquad \mathscr{T}^{\alpha-\gamma} = \begin{pmatrix} M_1 & 0 \\ 0 & M_2 \end{pmatrix}, \tag{4c}$$

$$\mathscr{S} = \begin{pmatrix} 1 & 0 \\ \frac{1}{2}A & 1 \end{pmatrix}, \qquad I_- = \begin{pmatrix} 1 & 0 \\ 0 & -1 \end{pmatrix}. \tag{4d}$$

The matrices involved in this formulation are given by the expressions [6, 20],

$$[A(u)]_{ij} = 2\left\langle \phi_i(v;u) \left| \frac{\partial}{\partial u} \phi_j(v;u) \right\rangle \right., \tag{5}$$

$$[B(u)]_{ij} = [b(u)]_{ij} + \left\langle \phi_i \left| \frac{\partial^2}{\partial u^2} \phi_j \right\rangle \right., \tag{5a}$$

$$[b(u)]_{ij} = \frac{2\mu}{\hbar^2} \left\langle \phi_i \left| \eta^2 \left\{ E - \frac{1}{2}[\varepsilon_i(u) + \varepsilon_j(u)] \right.\right.\right.$$

$$\left.\left.\left. - [V(u,v) - V_0(u,v)] \right\} \right| \phi_j \right\rangle - \frac{3}{4\sigma^2}\delta_{ij}, \tag{5b}$$

$$[C_k]_{ij} = \langle \phi_i^P(v; u^{P-C} | \eta^{(-1)^k/2} | \phi_j^C(v; u^{P-C}) \rangle, \tag{6}$$

$$[M_k]_{ij} = \left\langle \phi_i^\alpha(v_\alpha; u_\alpha = 0) \left| \left(\frac{\eta_\alpha}{\eta_\gamma}\right)^{(-1)^k/2} \right| \phi_j^\gamma(v_\gamma; u_\gamma = 0) \right\rangle \qquad \text{for } k = 1, 2, \tag{7}$$

where $\langle\ \rangle$ means integration over the vibrational coordinate and $V_0(u, v)$ is the potential defining the vibrational basis employed, i.e.,

$$\left[-\frac{\hbar^2}{2\mu}\frac{d^2}{dv^2} + V_0(u,v) \right] \phi_i(v;u) = \varepsilon_i(u)\, \phi_i(v;u). \tag{8}$$

The channel and the region labels are given where quantities for both channels or for both regions of a given channel occur in one formula. The matrix A is skew-symmetric as a result of the assumed orthonormality and reality of the basis functions, $A^T = -A$, and vanishes at asymptotic arrangement channel boundaries, u_a^∞, $a = \alpha, \gamma$, where these functions are required to become independent of the u-coordinate (the first and the second derivatives are zero):

$$\lim_{u \to u_a^\infty} A(u) = 0. \tag{9}$$

If the basis is complete the matrices C_k and M_k for $k = 1, 2$, satisfy the relations:

$$C_1^T = C_2^{-1}, \qquad M_1^T = M_2^{-1}, \tag{10}$$

and the following formula holds for the matrix B,

$$B = b + \frac{1}{2}\frac{d}{du}A + \frac{1}{4}A^2. \tag{11}$$

The matrix b becomes constant and diagonal at the asymptotic boundaries:

$$\lim_{u \to u_a^\infty} [b(u)]_{ij} = [(k^a)^2]_{ij} = (k_j^a)^2\, \delta_{ij} \qquad \text{for} \quad a = \alpha, \gamma, \tag{12}$$

where $k_j^a = |k_j^a|$ for open and $k_j^a = i|k_j^a|$ for closed vibrational channel j (in the arrangement channel a). The matrix I_- in Eq. (4b) accounts for the change of sign of the $(\partial/\partial u)$-derivative at the α-γ boundary.

To complete the specification of the problem we have to define the solutions of physical interest as those which grouped in the two matrices $F_\alpha(u)$ and $F_\gamma(u)$ satisfy the scattering boundary conditions:

$$\begin{pmatrix} F_\alpha(u_\alpha^\infty) & F_\gamma(u_\alpha^\infty) \\ F_\alpha(u_\gamma^\infty) & F_\gamma(u_\gamma^\infty) \end{pmatrix} = \begin{pmatrix} \mathbf{O}_\alpha^* & 0 \\ 0 & \mathbf{O}_\gamma^* \end{pmatrix} - \begin{pmatrix} \mathbf{O}_\alpha & 0 \\ 0 & \mathbf{O}_\gamma \end{pmatrix} \begin{pmatrix} S_{\alpha\leftarrow\alpha} & S_{\alpha\leftarrow\gamma} \\ S_{\gamma\leftarrow\alpha} & S_{\gamma\leftarrow\gamma} \end{pmatrix}, \tag{13}$$

where $\mathbf{O}_a = |k^a|^{-1/2} \exp(ik^a u_a^\infty)$ for $a = \alpha, \gamma$, and $\begin{pmatrix} S_{\alpha\leftarrow\alpha} & S_{\alpha\leftarrow\gamma} \\ S_{\gamma\leftarrow\alpha} & S_{\gamma\leftarrow\gamma} \end{pmatrix}$ represents the arrangement channel decomposition of the scattering matrix S. The subscript of the solution matrix F denotes the initial channel. The information sought is the matrix of probabilities,

$$P = \begin{pmatrix} P_{\alpha\leftarrow\alpha} & P_{\alpha\leftarrow\gamma} \\ P_{\gamma\leftarrow\alpha} & P_{\gamma\leftarrow\gamma} \end{pmatrix},$$

for all transitions energically allowed in the process:

$$(P_{a\leftarrow a'})_{ij} = |(S_{a\leftarrow a'})_{ij}|^2 \qquad \text{for} \quad a, a' = \alpha, \gamma. \tag{14}$$

$$N_a^{\text{op}} \times N_{a'}^{\text{op}}$$

N_a^{op} denotes the number of open vibrational channels in the arrangement channel a.

Beside the nondiabatic representation chosen above (Eq. (2)) for the presentation of the problem, two other representations, namely the diabatic and the quasidiabatic representations, will be also used for finding the numerical solution by the algorithms given in the next section. In the remainder of this section we collect the formulas necessary to switch between the considered representations. The diabatic counterpart of $\mathscr{F}(u)$, denoted by $\mathscr{F}_{\bar{u}}(u) = \begin{pmatrix} f_{\bar{u}}(u) \\ (d/du) f_{\bar{u}}(u) \end{pmatrix}$, is generated through the relation,

$$\mathscr{S}(u)\, \mathscr{F}(u) = T(u; \bar{u})\, \mathscr{F}_{\bar{u}}(u), \tag{15}$$

which involves the orthogonal transform $T(u; \bar{u}) = \begin{pmatrix} t(u; \bar{u}) & 0 \\ 0 & t(u; \bar{u}) \end{pmatrix}$ defined as the solution to the problem

$$\left[\frac{d}{du} + \frac{1}{2} A(u)\right] t(u; \bar{u}) = 0, \qquad t(\bar{u}; \bar{u}) = 1, \tag{16}$$

where $\bar{u}$ is a fixed point. Thus, $\mathscr{F}_{\bar{u}}(u)$ satisfies the equation

$$\frac{d}{du} \mathscr{F}_{\bar{u}}(u) = \begin{pmatrix} 0 & 1 \\ -b_{\bar{u}}(u) & 0 \end{pmatrix} \mathscr{F}_{\bar{u}}(u), \tag{17a}$$

where

$$b_{\bar{u}}(u) = t^{T}(u; \bar{u})\, b(u)\, t(u; \bar{u}). \tag{17b}$$

The conversion of $\mathscr{F}(u)$ to the quasidiabatic representation can be described as the following two-step procedure:

$$\mathscr{S}(u)\, \mathscr{F}(u) = \sum_{i} \theta(u_i - u)\, \theta(u - u_{i-1})\, T(u; \bar{u}_i)\, \mathscr{F}_{u_i}(u) \tag{18a}$$

$$\simeq \sum_{i} \theta(u_i - u)\, \theta(u - u_{i-1})\, T(u; \bar{u}_i)\, D(i)\, \mathscr{F}(u; i), \tag{18b}$$

where

$$\bar{u}_i = (u_i + u_{i-1})/2, \qquad D(i) = \begin{pmatrix} d(i) & 0 \\ 0 & d(i) \end{pmatrix},$$

and $\theta(u)$ is the step function: $\theta(u) = 1$ for $u \geqslant 0$ and $\theta(u) = 0$ for $u < 0$. The first step, Eq. (18a), is the conversion to a sequence of diabatic representations defined differently for different sectors $[u_{i-1}, u_i]$ of the u-coordinate. The functions $\mathscr{F}(u; i)$, for $i = 1, 2, \ldots$, constituting the quasidiabatic representation are introduced in the second (approximate) step as solutions of the equations;

$$\frac{d}{du}\mathscr{F}(u; i) = \begin{pmatrix} 0 & 1 \\ -k^2(i) & 0 \end{pmatrix} \mathscr{F}(u; i) \qquad \text{for} \quad u \in [u_{i-1}, u_i]. \tag{19a}$$

The matrices $k^2(i)$ occurring in these equations and the matrices $d(i)$ occurring in Eq. (18b) result from the diagonalization of the matrices $b_{\bar{u}_i}(\bar{u}_i) = b(\bar{u}_i)$ for $i = 1, 2, \ldots$;

$$d^{T}(i)\, b(\bar{u}_i)\, d(i) = k^2(i).$$

Inserting the conversion relations, Eq. (15) or (18b), into one or into both sides of the continuity conditions (4a) and (or) (4b) we can find easily the modified $\mathscr{T}^{P-C}$ and $\mathscr{T}^{\alpha-\gamma}$-matrices necessary to match solutions generated in different representations in different regions of the integration range. Additional continuity conditions, at the boundaries of sectors, arise in the quasidiabatic representation,

$$\mathscr{F}(u_i; i+1) = \mathscr{O}(i+1; i)\, \mathscr{F}(u_i; i), \tag{20}$$

where

$$\mathscr{O}(i+1; i) = D^{T}(i+1)\, T(\bar{u}_{i+1}; \bar{u}_i)\, D(i).$$

The matrices $\mathscr{O}(i+1; i) = \begin{pmatrix} o(i+1; i) & 0 \\ 0 & o(i+1; i) \end{pmatrix}$ become the overlap matrices between the local bases of subsequent sectors, i.e.,

$$o(i+1; i) = d^{T}(i+1) \langle \Phi(v; u_{i+1})\, \Phi^{T}(v; u_i) \rangle\, d(i), \tag{20a}$$

if the basis Φ is complete [21].

3. Application of the $\mathscr{L}$-Matrix Approach

The $\mathscr{L}$-matrix approach to solving the coupled equations for inelastic and reactive scattering has been basically established in papers [11] and [12]. Some complementary remarks on symmetry of $\mathscr{L}$-matrices for equations in nondiabatic representations are given in Appendix B. Thus, here we confine ourselves to a schematic presentation of this approach which is aimed at introducing of a convenient notation. The aspects to be visualized in such notation are:

(1) the division of the integration range $[u_\alpha^\infty, u_\gamma^\infty]$ which is induced by two factors:

(a) the specific construction of the coordinate system, i.e., the division of $[u_\alpha^\infty, u_\gamma^\infty]$ into the arrangements channels, the polar and the Cartesian region;

$$[u_\alpha^\infty, u_\gamma^\infty] = [u_\alpha^\infty, u_\alpha^0 = 0] + [u_\gamma^0 = 0, u_\gamma^\infty]$$
$$= [u_\alpha^\infty, u_\alpha^{P-C}] + [u_\alpha^{P-C}, u_\alpha^0] + [u_\gamma^0, u_\gamma^{P-C}] + [u_\gamma^{P-C}, u_\gamma^\infty],$$

(b) requirements of numerical integration, i.e., a further division of each region into small sectors $[u_i, u_{i+1}]$ for $i = 1, 2, \ldots,$

(2) the shape (i.e., the representation) of the coupled equations actually integrated.

Without writing the detailed (and lengthy) formulas we present the $\mathscr{L}$-matrix approach as a consequent reformulation of the standard (Ω-matrix) approach to the coupled equations and as a useful tool in this respect we exploit the matrix operation $\hat{L}$ introduced in [12] (see also Appendix A).

The relation underlying the $\mathscr{L}$-matrix formalism is the definition of an $\mathscr{L}$-matrix corresponding to a given standard propagator $\Omega(u'', u')$;

$$\mathscr{L}(u', u'') = \hat{L}[I^- \Omega(u'', u')], \qquad I^- = \begin{pmatrix} -1 & 0 \\ 0 & 1 \end{pmatrix}. \tag{21}$$

Concerning the standard propagators for the coupled equations specified in the previous section, one point seems to be worth mentioning. Namely, in order to ensure uniform symmetry properties of the $\mathscr{L}$-matrices in all representations considered we make a little "unusual" choice of the Ω-propagator for the coupled equations (3). Instead of propagating the solution vectors $\mathscr{F}(u)$ (Eq. (3a)) we consider the propagation of the vectors $G(u) = \binom{f(u)}{g(u)} = \mathscr{S}(u)\,\mathscr{F}(u)$,

$$G(u'') = \Omega(u'', u')\, G(u'). \tag{22}$$

In the cases of the diabatic and the quasidiabatic equations, (Eqs. (17a) and (19a)), we deal directly with the solutions $\mathscr{F}_{\tilde{u}}(u)$ and $\mathscr{F}(u; i)$. The Ω-matrices for propagation of these solutions are denoted by $\Omega_{\tilde{u}}(u'', u')$ and $\tilde{\omega}(i, i-1)$, respec-

tively. $\tilde{\omega}(i, i-1)$ propagates between endpoints of ith sector, i.e., $u' = u_{i-1}$ and $u'' = u_i$.

The structure of the $\mathscr{L}$-matrix formalism in its application to Eqs. (3), (4) is shown in Table I. The "addition" relations for the $\mathscr{L}$-type propagators given in this table can be checked by making use of the properties of the $\hat{L}$-operation listed in Appendix A. All the Ω-type propagators fulfill the condition of J_--unitarity, Eq. (B11), and consequently all the $\mathscr{L}$-type matrices are symmetric. The J_--unitarity of the sector and region Ω-propagators results from the properties of the coupling matrices in Eq. (3). In the case of the global and the channel propagators, $\mathbf{\Omega}$ and Ω^a, $a = \alpha, \gamma$, this unitarity reflects also the properties of the matching matrices (Eq. (10)).

Obviously, the global Ω-propagator, $\mathbf{\Omega}$, and hence the global $\mathscr{L}$-propagator, $\mathbf{L}$, are related to the scattering matrix S. After some inspection of the formulas given in Table I in conjunction with the formulas (21) and (22) we find that the matrix $\mathbf{L}$ propagates the solutions of Eq. (3) in the following way:

$$I_- \begin{pmatrix} g(u_\alpha^\infty) \\ g(u_\alpha^\infty) \end{pmatrix} = \mathbf{L} I_- \begin{pmatrix} f(u_\alpha^\infty) \\ f(u_\gamma^\infty) \end{pmatrix}.$$

Remembering that the matrix A involved in the definition of g, (Eqs. (22), (4d)), vanishes at the points u_α^∞ and u_γ^∞ and applying the above relation to the solutions F_α and F_γ (Eq. (13)) and their derivatives we derive the necessary formula for the matrix S,

$$S = W^{-1} W^*, \tag{23}$$

TABLE I

Ω- and $\mathscr{L}$-Type Propagators of Solutions of Eqs. (3), (4)

$[u', u'']$	$\Omega(u'', u')$ (Eq. (22))	$\mathscr{L}(u', u'')$ (Eq. (21))
sector $[u_{i-1}, u_i]$	$\omega(i, i-1)$	$l(i-1, i)$
i sectors $[u_0, u_i]$	$\omega(i, 0) = \omega(i, i-1)\,\omega(i-1, 0)$	$l(0, i) = \hat{L}[\hat{L}[l(i-1, i)]\, I^{-}\, \hat{L}[l(0, i-1)]]$
polar region, P_a $[u_a^0, u_a^{P-C}]$	$\boldsymbol{\omega}^{P_a}$	$\mathbf{l}^{P_a}$
Cartesian region, C_a $[u_a^{P-C}, u_a^\infty]$	$\boldsymbol{\omega}^{C_a}$	$\mathbf{l}^{C_a}$
channel a, $a = \alpha, \gamma$	$\Omega^a = \boldsymbol{\omega}^{C_a} \mathscr{T}^{C\ \ P} \boldsymbol{\omega}^{P_a\ \ a}$	$L^a = \hat{L}[\hat{L}[\mathbf{l}^{C_a}]\, \mathscr{T}^{C-P} I^- \hat{L}[\mathbf{l}^{P_a}]]$
entire range $[u_\alpha^\infty, u_\alpha^\infty]$	$\mathbf{\Omega} = I_- \Omega^\gamma \mathscr{T}^{\gamma-\alpha} I_- (\Omega^\alpha)^{-1\ \ a}$	$\mathbf{L} = -\hat{L}[\hat{L}[L^\gamma]\, \mathscr{T}^{\gamma-\alpha} I^- \hat{L}[J L^\alpha J]]$

[a] $\mathscr{T}^{C-P} = (\mathscr{T}^{P-C})^{-1}$, $\mathscr{T}^{\gamma-\alpha} = (\mathscr{T}^{\alpha-\gamma})^{-1}$, see Eq. (4c).

where

$$W = I\_\mathbf{L}I\_\mathbf{O} - \dot{\mathbf{O}},$$

$$\mathbf{O} = \begin{pmatrix} \mathbf{O}_\alpha & 0 \\ 0 & \mathbf{O}_\gamma \end{pmatrix}, \qquad \dot{\mathbf{O}} = \begin{pmatrix} \dfrac{d}{du_\alpha}\mathbf{O}_\alpha & 0 \\ 0 & \dfrac{d}{du_\gamma}\mathbf{O}_\gamma \end{pmatrix}.$$

The structure of propagators shown in Table I is applicable in principle also to the equations obtained after conversion to the diabatic and quasiadiabatic representations. The $\mathscr{L}$-type propagators for these equations are denoted, as the Ω-type propagators before, by the subscript "$\bar{u}$" and by tilda, respectively. Obviously, the matching transformations $\mathscr{T}^{P-C}$ and $\mathscr{T}^{\alpha-\gamma}$ should be modified appropriately (see the end of Sect. 2). The relation for the accumulation of the sector $\mathscr{L}$-propagators in the quasiadiabatic involves additionally the overlap matrices $\mathscr{O}$ and reads

$$\tilde{l}(0, i) = \hat{L}[\hat{L}[l(i-1, i)]\, \mathscr{O}(i; i-1)\, I^{-}\hat{L}[l(0, i-1)]]. \tag{24}$$

The way of linking the $\mathscr{L}$-matrix formalism to computational practice is obvious. Combining a procedure for estimation of the sector $\mathscr{L}$-propagators with the "addition" relations listed in Table I we will get an algorithm for finding the propagator $\mathscr{L}$ in any desired part of the integration range. A variety of such procedures can be derived, of course, by applying either the approximate solution or the approxmate potential approach [1]. We list below the $\mathscr{L}$-matrix algorithm investigated in this paper—the approximate solution algorithm developed in [11, 12] as a generalization of the log-derivative method of Johnson [9]. It is applied to the present problem to give the region $\mathscr{L}$-propagator in the non-diabatic and in the diabatic representations. Thus, the following two versions of the algorithm are exploited:

(A) The nondiabatic version gives the matrix I

(1) Divide the region considered, $[u_a^0, u_a^{P\ C}]$ or $[u_a^{P\ C}, u_a^\infty]$, for $a = \alpha, \gamma$, into M sectors of length $2h$ and denote:

$$u_k = u_a^0 + kh \qquad \text{for} \quad k = 0, 1, 2, \ldots, 2M, \quad u_{2M} = u_a,$$

(2) Calculate matrices z, p, and r for the first sector

$$z_2 = 14 - 4h^2 b(u_2) - s_{0,2},$$

$$p_2 = w_{0,2},$$

$$r_2 = -7 + 2h^2 b(u_0) + t(u_0; u_2)\, s_{0,2}\, t^T(u_0; u_2).$$

(3) Add the subsequent sectors, i.e., calculate z_{k+2}, p_{k+2}, r_{k+2} for $k = 2, 4, 6, \ldots, 2M-2$,

$$z_{k+2} = 14 - 4h^2 b(u_{k+2}) - s_{k,k+2} - w_{k,k+2} y_{k+2} w_{k,k+2}^T,$$

$$p_{k+2} = p_k y_{k+2} w_{k,k+2},$$

$$r_{k+2} = r_k + p_k^T y_{k+2} p_k,$$

where

$$y_{k+2} = z_k - [t(u_k; u_{k+2})\, s_{k,k+2}\, t^T(u_k; u_{k+2})]^{-1},$$

$$s_{k,k+2} = \left[\frac{1}{4} - \frac{h^2}{8} t^T(u_{k+1}; u_{k+2})\, b(u_{k+1})\, t(u_{k+1}; u_{k+2})\right]^{-1},$$

$$w_{k,k+2} = (-1 + s_{k,k+2})\, t^T(u_k; u_{k+2}).$$

Determine the matrices $t(u; u_{k+2})$ at $u = u_k$, u_{k+1}, $u_{k+(3/2)} = u_k + (\frac{3}{2})h$ from the following formulas:

$$t(u_k; u_{k+2}) = \left[1 - \frac{h}{6} A(u_k)\right]^{-1} \left[1 + \frac{h}{6} A(u_{k+2}) + \frac{2h}{3} A(u_{k+1})\, t(u_{k+1}; u_{k+2})\right],$$

$$t(u_{k+1}; u_{k+2}) = \left[\frac{3}{8} - \frac{h}{32} A(u_{k+1})\right]^{-1} \left[-\frac{5}{8} - \frac{3}{32} hA(u_{k+2}) + t(u_{k+(3/2)}; u_{k+2})\right],$$

$$t(u_{k+(3/2)}; u_{k+2}) = \left[1 - \frac{h}{8} A(u_{k+(3/2)})\right]^{-1} \left[1 + \frac{h}{8} A(u_{k+2})\right].$$

(4) Calculate the matrix $\mathbf{I} = \begin{pmatrix} \mathbf{I}_1 & \mathbf{I}_2 \\ \mathbf{I}_3 & \mathbf{I}_4 \end{pmatrix}$

$$\mathbf{I}_1 = r_{2M}/h, \qquad \mathbf{I}_2 = -p_{2M}/6h,$$

$$\mathbf{I}_3 = \mathbf{I}_2^T, \qquad \mathbf{I}_4 = -[z_{2M} - 7 + 2h^2 b(u_{2M})]/6h.$$

(B) The diabatic version gives the matrix $\mathbf{I}_{\bar{u}}$. Here the addition proceeds by half sectors defined as in case (A):

$$z_0^{-1} = 0, \qquad p_1 = -\frac{1}{h}, \qquad r_1 = -\frac{1}{h} + \frac{h}{3} b_{\bar{u}}(u_0),$$

$$z_{k+1} = -6 + \left[0.125 + \frac{h^2}{48} b_{\bar{u}}(u_{k+1})\right]^{-1} - z_k^{-1}$$

$$\text{for} \quad k = 0, 2, 4, 6, \ldots, 2M-2,$$

$$z_{k+1} = 2 - \frac{2h^2}{3} b_{\bar{u}}(u_{k+1}) - z_k^{-1} \qquad \text{for} \quad k = 1, 3, 5, \ldots, 2M-1,$$

where

$$b_{\bar{u}}(u_k) = t^T(u_k; \bar{u})\, b(u_k)\, t(u_k; \bar{u}) \qquad \text{for} \quad k = 0, 1, 2, \ldots, 2M,$$

$$\left.\begin{aligned} p_{k+1} &= z_k^{-1} p_k \\ r_{k+1} &= r_k + h p_k^T p_{k+1} \end{aligned}\right\} \qquad \text{for} \quad k = 1, 2, 3, 4, \ldots, 2M-1$$

$$\mathbf{I}_{\bar{u}} = \begin{pmatrix} r_{2M} & p_{2M}^T \\ p_{2M} & [1 - (h^2/3)\, b_{\bar{u}}(u_{2M}) - z_{2M}]/h \end{pmatrix}.$$

Simultaneously with performing these operations the problem (16) is solved (by the Runge-Kutta algorithm with the step size h) in order to get the matrices $t(u_k; \bar{u})$ for $k = 0, 1, 2, \ldots, 2M$. A convenient choice of $\bar{u}$ is: $\bar{u} = u_0$. The obtained matrix $\mathbf{I}_{\bar{u}}$ can be converted, of course, to the matrix $\mathbf{I}$ (see Appendix B, Eq. (B12)).

Though there is no approximate potential algorithm derived originally from the $\mathscr{L}$-matrix formalism we can easily adapt to this formalism the "$\mathscr{R}$-matrix propagation" method of Light *et al.* [6-8]. Since the approximate potential approach is intrinsicly connected with the quasiadiabatic representation we use as working quantities the matrices $\tilde{I}$, $\tilde{\mathbf{I}}$, and $\tilde{L}$ defined above. These matrices as well as the global matrix $\tilde{\mathbf{L}}$ are related to the corresponding $\mathscr{R}$-matrices of Light's method [6] by the formula

$$\mathscr{L} = I_- \mathscr{R}^{-1} I_- . \tag{25}$$

The modifications implied by the change of the working quantities can be conveniently analysed by exploiting the properties of the operation $\hat{L}$ (Appendix A). Obviously, this operation is involved in the construction of the matrices $\mathscr{R}$ from the appropriate standard propagators. Substituting the expression: $\tilde{\mathbf{L}} = \tilde{L}[I^- \tilde{\mathbf{\Omega}}]$ for the left-hand side of (25) we get after some manipulations the following formula for the global $\mathscr{R}$-matrix;

$$\mathbf{R} = \hat{L}[I^- J \mathbf{\Omega} J], \qquad J = \begin{pmatrix} 0 & 1 \\ 1 & 0 \end{pmatrix}.$$

In the analogous way we can find also the respective formulas: for the channel $\mathscr{R}$-matrices, $R^a = \hat{L}[I^- J \tilde{\Omega}^a J]$, $a = \alpha, \gamma$, for the region $\mathscr{R}$-matrices,

$$\mathbf{r}^r = \hat{L}[I^- J \tilde{\omega}^r J] \qquad \text{for} \quad r = P_a, C_a, \; a = \alpha, \gamma,$$

and for the sector $\mathscr{R}$-matrices, $r(i-1, 1) = \hat{L}[I^- J \tilde{\omega}(i, i-1) J]$. It becomes apparent from these formulas that the simple renumbering of the blocks of the matrices $\tilde{\omega}$ in the original procedure for the sector propagators r suffices to make the procedure work as a generator of the sector propagators $\tilde{I}$. Moreover, the adaptation of the entire $\mathscr{R}$-matrix accumulation procedure to these propagators appears to be only a matter of interchanging the role of the matrices C_1 and C_2, and the matrices M_1 and M_2 in the matching transformations. The only other change concerns the final procedure for the matrix S which should be adjusted to the formula (23).

It should be noted that all the introduced modifications cannot affect the efficiency of the original method. This fact is consistent with the conclusion reached earlier [16] that there should be no practical difference between the $\mathscr{L}$- and $\mathscr{R}$-type propagators as long as the approximate potential is considered for their determination. Thus, the adaptation of the "$\mathscr{R}$-matrix propagation" method to the $\mathscr{L}$-matrix formalism has mainly an aesthetical justification: we wish to deal with the same propagators in all procedures used in the computational investigations. The goals and the results of the computations are reported in the next section.

4. Computational Investigations: Description of the Tests and Discussion of the Results

The questions of interest are:

(1) How do the approximate solution $\mathscr{L}$-matrix algorithms compare with the approximate potential, i.e., the "$\mathscr{R}$-matrix propagation," algorithm in respect of accuracy and speed in solving a problem typical for the considered group of collision processes.

(2) To what degree can the quality of the "$\mathscr{R}$-matrix propagation" method be enhanced by a combination with the approximate solution $\mathscr{L}$-matrix algorithms.

Intending to answer these questions, at least in part, we created and tested the following modified versions of the *RXN1D* program [5]:

(1) the approximate potential version (AP) which is the $\mathscr{L}$-matrix adaptation of the original program,[1]

[1] The step-predicting algorithm in this program is designed, as described in the original papers on the "$\mathscr{R}$-matrix propagation" method [6, 7], to keep control over the first correction term to the Magnus approximation (this is the approximation made in Eq. (19a)) and over the rate of change of the quasiadiabatic basis. The coded formulas for the size of the $(i+1)$-th sector, $h_{i+1} = u_{i+1} - u_i$, are

$$\tilde{h}_{i+1} = \text{BSTEP}/[b'(i)]^{1/3}, \qquad \tilde{\tilde{h}}_{i+1} = h_i\text{*CUPMAX}/|[\mathscr{C}(i; i-1)]_{1,2}|,$$

where

$$b'(i) = \frac{2\mu}{\hbar^2}\left\{[\Delta_i(\eta_0^2 V_0)]^2 + \frac{\hbar^2}{4}[\Delta_i(\eta_0^2\omega)]^2\right\}^{1/2},$$

$$\Delta_i(\eta_0^2 V_0) = [\eta^2(v_{\min}^i)\, V(\bar{u}_i, v_{\min}^i) - \eta^2(v_{\min}^{i-1})\, V(\bar{u}_{i-1}, v_{\min}^{i-1})]/(\bar{u}_i - \bar{u}_{i-1}),$$

$v_{\min}^i$ is the position of the minimum of $V(\bar{u}_i, v)$ and $\bar{u}_i$ is the midpoint of the ith sector. $\Delta_i(\eta_0^2\omega)$ is defined analogously to $\Delta_i(\eta_0^2 V_0)$ and $\omega(\bar{u}_i) = [(d/dv^2)\, V(\bar{u}_i, v_{\min}^i)/\mu]^{1/2}$. h_{i+1} is finally chosen as $\min(\tilde{h}_{i+1}, \tilde{\tilde{h}}_{i+1})$ and is required to be in the [STPMIN, STPMAX] interval. CUPMAX, BSTEP, STPMIN, and STPMAX are input parameters. In our tests: STPMIN = 0.01 bohr, STPMAX = 1 bohr, CUPMAX ranged from 0.12 to 0.03 and BSTEP ranged from 10^{-4} to 10^{-5}.

(2) the approximate solution versions, ASnd and ASd, in which the generalized log-derivative algorithms, the nondiabatic version and the diabatic version, respectively, are used in all regions of the reaction coordinate.

(3) the hybrid versions, ASnd-AP and ASd-AP, in which the respective approximate solution algorithms are used in the polar regions only.

It seems appropriate to give some details on how the approximate solution algorithms were implemented into the *RXN1D* program. First, some steps were needed to account for the change of the wavefunction representation. To exploit the procedures of the original program to possibly high degree we chose the nondiabatic basis in the form of perturbed harmonic oscillator eigenfunctions, i.e., we set

$$V_0(u, v) = \tfrac{1}{2}\not{k}(u)[v - \tilde{v}(u)]^2 \qquad \text{in Eq. (8).}$$

With this choice the evaluation of the matrices b, C_k, and M_k for $k = 1, 2$, did not require any changes and the following simple formula could be used for the evaluation of the matrix A,

$$A(u) = \frac{1}{2\beta(u)} \frac{d}{du} \beta(u)\, a_\beta - \sqrt{2\mu\beta(u)/\hbar}\, \frac{d}{du} \tilde{v}(u)\, a_{\tilde{v}},$$

where

$$(a_\beta)_{ij} = -(a_\beta)_{ji} = \delta_{i,j-2} \sqrt{(i+1)(i+2)},$$
$$(a_{\tilde{v}})_{ij} = -(a_{\tilde{v}})_{ji} = \delta_{i,j-1} \sqrt{i+1} \qquad \text{for} \quad i, j = 0, 1, 2, 3, \ldots,$$
$$\beta = \sqrt{\not{k}/\mu}$$

The variable potential parameters, $\not{k}(u)$ and $\tilde{v}(u)$, we determined as polynomial approximations to the values $\not{k}(u_i)$ and $\tilde{v}(u_i)$ obtained by the procedure that fits parabolas to the *A-B-C* potential surface in the original *RXN1D* program. The points u_i were chosen as equidistant points covering a given region of the reaction coordinate. Planning to use eventually the nondiabatic representation in the polar regions only we forced the first and the second derivatives of $\not{k}(u)$ and $\tilde{v}(u)$ to vanish at the polar-Cartesian boundaries. The polynomial coefficients for $\not{k}(u)$ and $\tilde{v}(u)$ determined in this way served also to calculate the parameters of the quasiadiabatic basis for the approximate potential algorithm.

Obviously, hoping to improve the *RXN1D* program by introducing the approximate solution algorithms we had to keep in mind the overall usefulness of the program in serial calculations. Therefore, while coding these algorithms we tried to make possibly large savings in computer time needed in second (and further) energy calculations for a given collision system. Exploiting the energy independence of the first derivative coupling matrix we excluded from these calculations the operations of the evaluation of the transformations t in both algorithms. Following

the original program we simplified also the evaluation of the coupling matrix b by applying the formula

$$b(u; E) = b(u; E_{\text{ref}}) + (E - E_{\text{ref}})\,\tilde{b}(u)$$

in which $E\tilde{b}(u)$ is the energy dependent part of b (see Eq. (5b)) and E_{ref} denotes the energy in the first energy calculation. An analogous formula was used also for the matrix $b_{\bar{u}}$. Some necessary matrices should be stored, of course, in the first energy calculation. These are the matrices $b(u_k)$, $\tilde{b}(u_k)$ for $k = 0, 1, 2, \ldots, M$, and $t(u_k; u_{k+2})$, $t(u_{k+1}; u_{k+2})$ for $k = 0, 2, 4, 6, \ldots, M-2$, in the case of the algorithm A (the nondiabatic version) and the matrices $b_{\bar{u}}(u_k)$, $\tilde{b}_{\bar{u}}(u_k)$ for $k = 0, 1, 2, \ldots, M$, and $t(u_M; \bar{u})$ in the case of the diabatic version.

With the same purpose of speeding up serial calculations we considered also the possibility of incorporating into the approximate solution algorithms a procedure analogous to the basis contraction in the "$\mathscr{R}$-matrix propagation" method. The procedure consists in reducing the dimension of the problem by using only appropriate blocks of all matrices stored in first energy calculation. For similar reasons as in the original *RXN1D* program this basis contraction could be expected to work within the nondiabatic version of the log-derivative algorithm. It must fail, however, when the diabatic version is used.

To keep the storage requirements on a reasonable level we did not include the second energy facilities into the purely approximate solution versions of the program.

Now we proceed to the presentation of the computational material which has been collected to characterize the performance of the modified versions of the *RXN1D* program. This material concerns solving of the coupled equations for the $H + H_2$ collinear reaction on the Porter–Karplus potential surface [17]. Some tests were performed also on the $F + H_2$ reaction on the Muckerman-5 potential surface [18]. The form of our presentation is chosen to expose the features of primary importance for a comparison of the approximate solution and the approximate potential approaches; i.e., convergence properties with respect to sector width and computational effort required at one sector. We paid less attention to the convergence with respect to the basis set length because we did not expect this feature to be significant for assessing relative effectiveness of the methods tested. We were, however, indirectly concerned with this convergence when we examined the basis contraction procedure.

In our studies of the convergence properties we measured the accuracy of an individual calculation by the r.m.s. fractional error, ρ, of the transition propability matrix, P, which was calculated according to the formula:

$$\rho = (N_{\text{op}}^2 - N_{\text{op}})^{-1} \left\{ \sum_{a,a'=\alpha,\gamma} \sum_{i=1}^{N_a^{\text{op}}} \sum_{j=1}^{N_{a'}^{\text{op}}} \left[1 - \frac{(P_{a \leftarrow a'})_{ij}}{(\tilde{P}_{a \leftarrow a'})_{ij}} \right]^2 (1 - \delta_{aa'}\delta_{ij'}) \right\}^{1/2},$$

where

$$N_{\text{op}} = N_{\alpha}^{\text{op}} + N_{\gamma}^{\text{op}}.$$

As the reference values, $(\tilde{P}_{a \leftarrow a'})_{ij}$ for $a, a' = \alpha, \gamma$, we used the results of the most accurate calculation done for a given set of coupled equations. The reference calculations for the error estimations given in this paper are summarized in Tables II and III.

We start the analysis of the information obtained from our investigations with a discussion of the accuracy of the results yielded by the modified versions of the *RXN1D* program.

The r.m.s. fractional errors of the transition probability matrices for the $H + H_2$ system calculated with each version at several energies are shown in Fig. 1 as functions of the number of sectors used for solving the coupled equations in the fixed integration range. An analogous error plot for the $F + H_2$ system is made in Fig. 2. The overall picture of the relative accuracy of the methods is generally consistent with what is well known on the properties of the appr. solution and the appr. potential approaches from their applications to inelastic (nonreactive) scattering calculations. At low energies and for a given number of sectors both the ASnd and ASd versions give more accurate results than the AP version (Fig. 1a). The differences diminish when the energy grows (Fig. 1d). The AS versions work usually

TABLE II

Accurate Solutions of the Test Problems $H_2 + H \rightleftarrows H + H_2$ Reaction on the Porter–Karplus Potential Surface [17]

Test No.	Energy[a] E (eV)	No. of channels N	Probability matrix[b] $P_{\alpha \leftarrow \alpha}$		$P_{\gamma \leftarrow \alpha}$			
1	0.87060	10	0.41016	0.18030		0.18228	0.22726	
			0.18030	0.46419		0.22726	0.12825	
2	0.89760	10	0.03214	0.12389		0.66320	0.18077	
			0.12389	0.40271		0.18077	0.29264	
3	0.89760	12	0.03214	0.12390		0.66323	0.18073	
			0.12390	0.40287		0.18073	0.29250	
4	1.0	10	0.07666	0.08841		0.59624	0.23868	
			0.08841	0.16381		0.23868	0.50909	
5	1.3966	12	0.25836	0.21258	0.06732	0.12986	0.25313	0.07875
			0.21258	0.12315	0.05516	0.25313	0.25214	0.10384
			0.06732	0.05516	0.21204	0.07875	0.10384	0.48288

6 $F + H_2 \rightleftarrows FH + H$ reaction on the Muckerman-5 potential surface [18]
$E = 1.75$ eV, $N = 12$

$P_{\alpha \leftarrow \alpha}$		$P_{\gamma \leftarrow \alpha}$			$P_{\gamma \leftarrow \gamma}$			
0.65134	0.00099(−2)	0.00114	0.08406	0.26345	0.98182	0.01812	0.00047(−1)	0.00274(−3)
					0.01812	0.97533	0.05013(−1)	0.00399(−1)
					0.00047(−1)	0.05013(−1)	0.87147	0.03941
					0.00274(−3)	0.00399(−1)	0.3941	0.69673

[a] Energy is measured from the bottom of the potential valley in the asymptotic γ (exit) channel.
[b] The probabilities are correct to all except the last significant figure shown.

TABLE III

Some Details on Calculation of the Probabilities Shown in Table II

Test No.	Method	Number of sectors[a] M $(M_\alpha^r, M_\alpha^c, M_\gamma^r, M_\gamma^c)$[b]
1–3	ASnd	371 (118, 253, —, —)[c]
4, 5	ASnd	557 (177, 380, —, —)
6	ASd	588 (98, 157, 112, 221)

[a] The length of sectors is $2h$. $h = 0.0075$ bohr in tests 1–3, 6 and $h = 0.005$ bohr in test 4, 5.

[b] M_c^r denotes the number of sectors used in the region r (Polar or Cartesian) of the arrangement channel c ($c = \alpha, \gamma$).

[c] It sufficies to integrate the coupled equations for the symmetric $H + H_2$ reaction in one arrangement channel only.

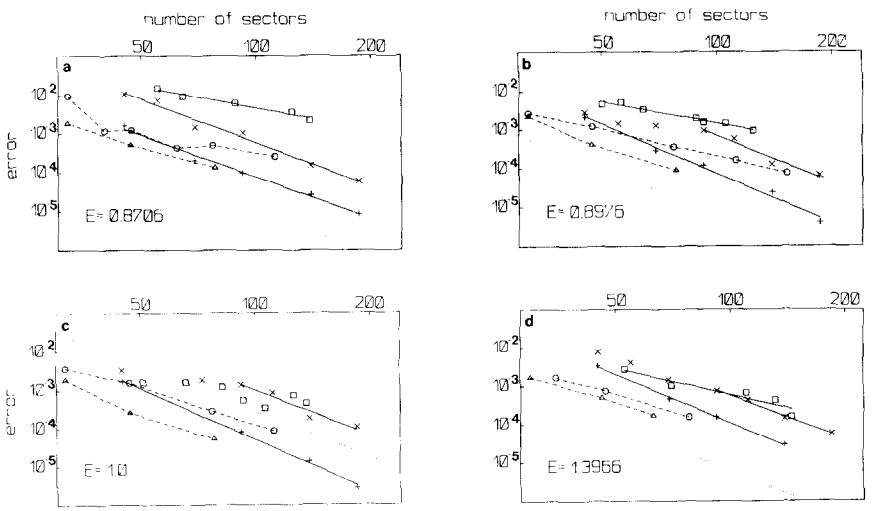

FIG. 1. Errors of the propability matrices for the $H + H_2$ reaction (test problems no. 1, 2, 4, 5 in Table II) obtained by the AP (□), ASnd (×), ASd (+), ASnd-AP (○), and ASd-AP (△) methods versus the number of sectors used (M). The dotted lines show perfect M^{-4} rate of convergence.

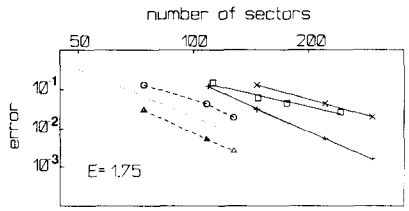

FIG. 2. Same as in Fig. 1 for the $F+H_2$ system (test problem no. 6 in Table II).

better within higher accuracy regime. Of course, the hybrid versions deserve most attention. These versions yield results that are about 10 times more accurate than those obtained with the AP version when the same number of sectors is used. They are also better than these of the AS versions if not too high accuracy is required.

To visualize the origins of this superiority of the hybrid versions we give more details on the performance of the algorithms constituting them in different regions of the integration range. In Fig. 3 we present an accuracy comparison of the AS and the AP algorithms in solving the coupled equations in the polar and in the Cartesian regions. The error of the probability matrix is plotted versus the number of sectors which was varied in the specified region only. The second region was integrated "exactly," i.e., the same way as in the reference calculation (see Table III). As we see the AS algorithms excel the AP method considerably in the polar region. The AP algorithm becomes, however, superior in the Cartesian region.

Another measure of the performance of the AS and the AP algorithms is given in Figs. 4 and 5 by showing how the number of sectors necessary to integrate over a unit distance, i.e., dM/du, was changing along the integration range in the

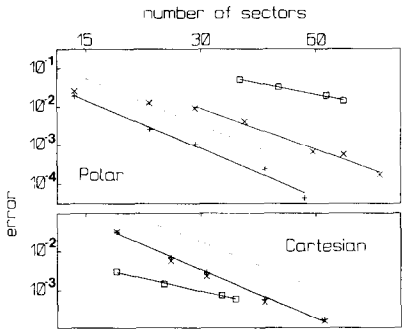

FIG. 3. Errors of the probability matrix for the $H+H_2$ reaction at $E=0.89760$ eV (test problem no. 2 in Table II) versus the number of sectors (M) used to integrate the coupled equations by the AP (□), ASnd (×), and ASd (+) methods in the region of the reaction coordinate specified in the corner of each panel. Outside this region the equations were integrated "exactly," i.e., by the ASnd method with the step size $h=0.0075$ bohr (see Table III). The dotted lines are "reference" M^{-4} lines.

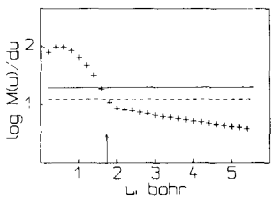

FIG. 4. Comparison of dM/du for the AP (+), ASnd (—), and ASd (---) methods in the 12 channel calculations for the $H+H_2$ reaction at $E=1.3966$ eV. The errors are given in Table V (case 4b). The arrow marks the polar-Cartesian boundary.

calculation which yielded the transition matrices of approximately the same accuracy. The quantity $dM(u)/du$ was evaluated from the formula

$$\frac{dM(u)}{du} \simeq \frac{M(u)-M(u-\Delta u)}{\Delta u},$$

where $M(u)$ denotes the number of sectors used to integrate over the interval $[0, u]$. Obviously, in the AS algorithms this quantity is constant and equal to $1/2h$ where h is the step size used. The fact to be noted is that the corresponding horizontal lines in Figs. 4 and 5 intersect the curves describing the AP algorithm near the polar-Cartesian boundaries. This is an indication that these boundaries are on average the best points for switching between the AS and the AP algorithms in the hybrid programs. Returning to Fig. 3 we would like to comment on the relative accuracy of the AS algorithms themselves. The figure shows clearly that both the ASnd and ASd algorithms perform almost identically in the Cartesian region. In the polar region the diabatic version is more accurate. For an explanation we have to refer to the derivation of these algorithms [11, 12] and remember that in both cases it was based on the same discretization procedure of the coupled equations obtained after the first derivative coupling had been eliminated. Different approximate ways, however, were applied to determine the transformation necessary for this elimination. Therefore the algorithms may differ in accuracy depending on the magnitude of the first derivative coupling. In the Cartesian regions this coupling is much smaller than in the polar regions. Apparently, it has negligible influence on the probability matrix in the case shown in Fig. 3.

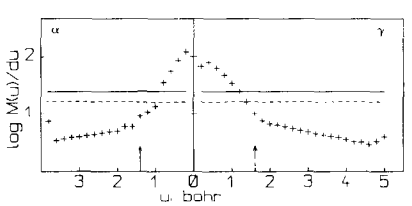

FIG. 5. Same as in Fig. 4 but for the $F+H_2$ calculations reported in Table VI. The letters in the upper corners denote the respective arrangement channels.

The solid lines are drawn in Fig. 3 as well as in Figs. 1 and 2 to exhibit the rate of convergence in the AS and in the AP methods with respect to the number of sectors used, M. The uniform M^{-4}- (or h^4) type convergence was always found in the diabatic version of the log-derivative algorithm. The convergence in the nondiabatic version of this algorithm must be, of course, somewhat affected by the less accurate treatment of the first derivative coupling. We noted a departure from the h^4 rate especially at larger values of h. In most tested cases the result obtained by the AP method converged at a rate definitely lower than M^{-4}.

To get an estimation of the rate of convergence in the hybrid versions we have to look at the broken lines in Fig. 1. It should be made clear, however, that only the best results obtained for a given number of sectors are joined by these lines.

In practice the convergence can be much less uniform. Some efforts must always be made to choose the optimal set of integration parameters in the polar and in the Cartesian regions, i.e., to achieve a tolerable accuracy with a minimal number of sectors. The average slopes of the broken lines give in fact the upper limits of the rate of convergence possible to obtain by the hybrid methods in the cases shown. In general, the convergence in the hybrid method does not reach the M^{-4} level.

Now we direct our considerations toward an estimation of the computational effort required by the tested versions of the *RXN1D* program to achieve a given accuracy of the results. To this end, we should add to what was stated above concerning the accuracy dependence on the number of sectors used in the AP and in the AS methods a comparison of the C.P.U. times spent at one sector. On the base of the tests made on the $H+H_2$ and $F+H_2$ systems we can compare average values of these times for the first and second energy calculations and for the number of coupled channels ranging from 5 to 12. This is done in Fig. 6. The unit used there is the time per sector needed to integrate the ten channel problem by the AP method at first energy. As expected, the relative differences in the C.P.U. time per sector encountered between the AP and the AS methods, applied to the rather

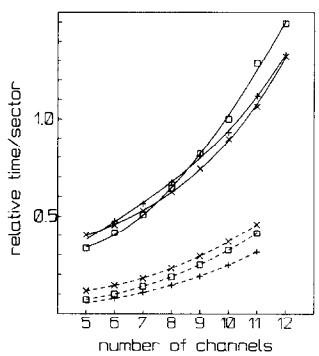

FIG. 6. C.P.U. times required at one sector by the AP (□), ASnd (×), and ASd (+) methods at first (—) and at second (---) energies vs the number of channels in the close coupled equations. All times shown are relative to the time per sector needed by the AP method in the 10 channel first energy calculation.

small problems, are not striking. They are of order of 10% for the ten channel problem at first energy. Somewhat larger are the differences between the AP and the ASd methods at second energies. This can perhaps be better seen from the numbers given in Table IV. This table exhibits also the slight differences, not shown in Fig. 6, between the times needed in the polar and in the Cartesian regions. Obviously, the times given in Table IV, and drawn in Fig. 6 do not measure rigorously the computational requirements of the tested methods. They do reflect, however, the quantitative relations holding in this respect. Namely,

(1) At first energy and in one sector both AS methods are less time-consuming than the AP method. For larger systems of coupled equations this is expected to become even more visible than in Fig. 6.

(2) At second energies the time requirements in the AP method are smaller than in the ASnd method but they remain larger than in the ASd method (about 1.3 times in the cases shown in Fig. 6).

The final comparison of the AP version of the *RXN1D* program with the AS and with the hybrid versions in respect to the efficiency in solving the test problems is made in Tables V and VI for some cases representative for our investigations. The efficiency is defined as one over the total C.P.U. time obtained after multiplying the numbers of sectors used (the third column) by the C.P.U. times given in Table IV. Obviously, with this definition one can compare calculations of the same level of accuracy only. The efficiency estimations given in Tables V and VI prove definitively the purposefulness of inserting the log-derivative algorithms into the *RXN1D* program. The gain in efficiency in both hybrid versions is visible in all reported cases. The best effect is achieved in the ASd-AP version which is about twice as efficient as the AP version in the first as well as in the second energy calculation. We can note also from these tables that the hydrid versions are better suited for more accurate calculations.

The last question we would like to answer concerns the applicability of the hybrid versions to serial calculations for one collision system at many energies. Though no proof of superiority of the ASnd-AP version to the ASd-AP version has

TABLE IV

Time[a] per Sector in First ($E1$) and Second ($E2$) Energy Calculations

Method	$N=10$ ($E1$)		$N=12$ ($E1$)		$N=10$
	Polar	Cart	Polar	Cart	($E2$)
AP	1.0	0.90	1.49	1.38	0.32
ASnd	0.90	0.88	1.32	1.25	0.37
ASd	0.93	0.92	1.33	1.27	0.25

[a] All times are relative to the time per sector needed by the AP method in the 10 channel first energy calculation.

TABLE V

Efficiency Comparison of the Methods in Solving the N-channel $H + H_2$ Problem at First ($E1$) and at Second ($E2$) Energy

Method	Error $\rho \times 10^3$	Number of sectors M (M^P, M^C)	Efficiency (C.P.U. time)$^{-1}$ [a]
Case 1. $E1 = 0.89760$ eV, $N = 10$			
AP	3.33	64 (47, 14)	1.0
ASnd	2.81	45 (14, 31)	1.5
ASd	2.17	45 (14, 31)	1.4
ASnd-AP	2.69	32 (14, 18)	2.1
ASd-AP	2.24	32 (14, 18)	2.0
Case 2. $E2 = 0.8960$ eV, $E1 = 1.0$ eV, $N = 10$			
AP	3.28	66 (49, 18)	2.8
ASnd-AP	2.69	32 (14, 18)	5.4
ASd-AP	2.24	32 (14, 18)	6.4
Case 3. $E1 = 1.0$ eV, $N = 10$			
(a) AP	1.59	51 (39, 12)	1.0
ASnd	1.68	45 (14, 31)	1.2
ASnd-AP	1.54	47 (29, 18)	1.2
ASd-AP	1.88	32 (14, 18)	1.7
(b) AP	0.336	106 (72, 34)	1.0
ASnd-AP	0.284	77 (59, 18)	1.5
ASd-AP	0.267	47 (29, 18)	2.4
Case 4. $E1 = 1.3966$ eV, $N = 12$			
(a) AP	2.73	53 (41, 12)	1.0
ASnd-AP	1.67	35 (22, 13)	1.6
ASd-AP	1.68	30 (17, 13)	1.9
(b) AP	0.160	145 (111, 34)	1.0
ASnd	0.144	139 (44, 95)	1.2
ASd	0.159	92 (29, 63)	1.8
ASnd-AP	0.156	78 (44, 34)	2.0
ASd-AP	0.174	63 (29, 34)	2.5

[a] The times are relative to the first energy calculations by the AP method.

TABLE VI

Efficiency Comparison of the Methods on the $F + H_2$ Problem

Method	Error ρ	Number of sectors M (M_α^P, M_α^C, M_γ^P, M_γ^C)	Efficiency (C.P.U. time)$^{-1}$ [a]
$E1 = 1.75$ eV, $N = 12$			
AP	0.044	175 (73, 11, 75, 16)	1.0
ASnd	0.044	220 (37, 58, 42, 83)	0.9
ASd	0.032	146 (24, 39, 28, 55)	1.4
ASnd-AP	0.044	108 (37, 12, 42, 17)	1.8
ASd-AP	0.030	74 (24, 9, 28, 13)	2.6

[a] See footnote in Table V.

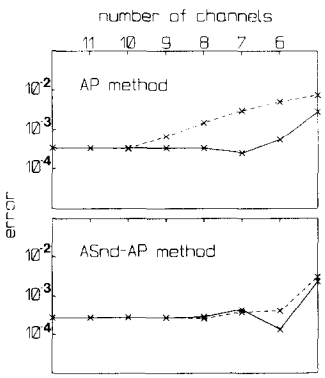

FIG. 7. Errors of the probability matrix for the $H+H_2$ reaction at $E=0.89760$ eV vs the number of channels propagated in the AP and in the ASnd-AP methods. The points joined by the solid lines concern the first energy calculations with uncontracted basis sets whereas the broken lines describe the convergence in the second energy calculations, but for $E2=E1$, with respect to the basis sets contracted from $N=12$ to P channels where P ranges from 11 to 5. The sectorization of the integration range (see footnotes [b] and [c] in Table III) was: $M=65$ ($M^P=48$, $M^C=17$) in the AP method and $M=32$ ($M^P=14$, $M^C=18$) in the ASnd-AP method.

been given so far there is a reason to expect that in serial calculations this version may be preferable. This is because of its ability to work with contracted bases.

The basis contraction could be a profitable procedure but, it should be said, that so far this is not a quite certain point yet. In fact there were some reports (e.g., [19]) about unsatisfactory convergence with respect to the contracted basis length in the original "$\mathscr{R}$-matrix propagation" method. However, we have found some evidence that after combining this method with the log-derivative algorithm the situation improves. For an example we refer to Fig. 7 which gives a comparison of convergence with respect to the uncontracted and to the contracted basis length in the AP version and in the hybrid ASnd-AP version of the *RXN1D* program. Looking at the solid lines in both panels of this figure we might expect that the 12 channel could be contracted to as few as 7 channels without causing any major deterioration of the results. This expectation is in fact confirmed in the hybrid version (the broken line is close to the solid line in the lower pannel) whereas in the AP version we observe a significant deterioration of the accuracy of the results obtained with contracted bases shorter than 10 channels.

Summarizing the findings of this work, particularly these concerning the performance of the hybrid versions of the *RXN1D* program; we can state that the approximate solution $\mathscr{L}$-matrix (i.e., the generalized log-derivative) methods make a significant contribution to the improvement of the numerical techniques available for quantum-mechanical investigations of reactive molecular collisions. Obviously, there are many different trends in these investigations and the range of computational requirements associated with them is wider than that covered in the present study.

In the continuation of the present work we plan to apply the hybrid methods to the reactive collision problems formulated in hyperspherical coordinates [24].

APPENDIX A. The Operation $\hat{L}$

The definition of $\hat{L}$:

$$\hat{L}[X]=\begin{pmatrix} -X_2^{-1}X_1 & X_2^{-1} \\ X_3-X_4X_2^{-1}X_1 & X_4X_2^{-1} \end{pmatrix}, \tag{A1}$$

where

$$X=\begin{pmatrix} X_1 & X_2 \\ X_3 & X_4 \end{pmatrix} \quad \text{and} \quad \det X_2 \neq 0.$$

The definition of $\hat{L}^T$

$$\hat{L}^T[X^T]=(\hat{L}[X])^T. \tag{A2}$$

Properties of $\hat{L}$:

(a) $\hat{L}\hat{L}[X]=X$,

(b) $\hat{L}[X^{-1}]=J\hat{L}[X]\,J$,

(c) $\hat{L}[JXJ]=(\hat{L}[X])^{-1}$, where $J=\left(\begin{smallmatrix} 0 & 1 \\ 1 & 0 \end{smallmatrix}\right)$.

(d) $\hat{L}[X\left(\begin{smallmatrix} T_1 & 0 \\ 0 & T_2 \end{smallmatrix}\right)]=\left(\begin{smallmatrix} T_2^{-1} & 0 \\ 0 & 0 \end{smallmatrix}\right)\hat{L}[X]\left(\begin{smallmatrix} T_1 & 0 \\ 0 & 1 \end{smallmatrix}\right)$, (A3)

(e) $\hat{L}[\left(\begin{smallmatrix} T_1 & 0 \\ 0 & T_2 \end{smallmatrix}\right)X]=\left(\begin{smallmatrix} 1 & 0 \\ 0 & T_2 \end{smallmatrix}\right)\hat{L}[X]\left(\begin{smallmatrix} 1 & 0 \\ 0 & T_1^{-1} \end{smallmatrix}\right)$, where T_k $(k=1,2)$ are nonsingular matrices.

APPENDIX B: On Symmetry of the $\mathscr{L}$-Matrix Approach to Coupled Equations in Nondiabatic Representation

Let us specify the objects of consideration in this section:

(1) the matrix differential equation;

$$\left[\frac{d^2}{du^2}+A(u)\frac{d}{du}+B(u)\right]\psi(u)=0. \tag{B1}$$

The $N\times N$ (real) matrices A and B are required to have the properties (which stand here for a definition of a nondiabatic representation):

$$A^T=-A, \qquad B=b+\frac{1}{2}\frac{d}{du}A+\frac{1}{4}A^2, \qquad b^T=b, \tag{B2}$$

(2) standard, or Ω-type, propagators of solutions of Eq. (B1). Under the term "standard propagator" we mean any $2N \times 2N$ matrix $\Omega(u, u') = \begin{pmatrix} \Omega_1 & \Omega_2 \\ \Omega_3 & \Omega_4 \end{pmatrix}$ which satisfies a first order differential equation equivalent to Eq. (B2), trough a transformation not involving, however, solutions of any other differential equations,[2] and the normalization condition: $\Omega(u', u') = 1$.

(3) $\mathscr{L}$-matrices, or $\mathscr{L}$-type propagators; $\mathscr{L} = \begin{pmatrix} \mathscr{L}^{(1)} & \mathscr{L}^{(2)} \\ \mathscr{L}^{(3)} & \mathscr{L}^{(4)} \end{pmatrix}$;

$$\mathscr{L}(u', u'') = \hat{L}[I^{-}\Omega(u'', u')], \qquad I^{-} = \begin{pmatrix} -1 & 0 \\ 0 & 1 \end{pmatrix}. \tag{B3}$$

First, we consider the most "obvious" choice of the standard propagator for Eq. (B1), namely the matrix $\Omega(u, u')$ satisfying the equations;

$$\frac{d}{du}\Omega(u, u') = \begin{pmatrix} 0 & 1 \\ -B & -A \end{pmatrix}\Omega(u, u'), \qquad \Omega(u', u') = 1, \tag{B4}$$

and we denote the corresponding $\mathscr{L}$-propagator by L. The following relation holds for Ω as a consequence of the properties of the matrices A and B, Eq. (B2),

$$\Omega^{T}(u'', u')\, U(u'')\, \Omega(u'', u') = U(u'), \tag{B5}$$

where

$$U(u) = \begin{pmatrix} A(u) & 1 \\ -1 & 0 \end{pmatrix}.$$

It can be shown that the corresponding relation for the matrix L reads [12],

$$L(u', u'') = L^{T}(u', u'') + \begin{pmatrix} -A(u') & 0 \\ 0 & A(u'') \end{pmatrix}. \tag{B6}$$

As an intermediate step in the proof we can use the following form of Eq. (B5) obtained by exploiting the properties (A2), (A3) of the operation $\hat{L}$:

$$\hat{L}^{T}[I_{-}\, L^{T}(u', u'')]\, U(u'')\, \hat{L}[L(u', u'')\, I_{-}] = U(u'), \qquad I_{-} = -I^{-}.$$

Thus, the matrix L is not symmetric. The relation (B6) suggests, however, construction of another symmetric matrix $\tilde{L}$;

$$\tilde{L}(u', u'') = L(u', u'') + \tfrac{1}{2}\begin{pmatrix} A(u') & 0 \\ 0 & -A(u'') \end{pmatrix}, \tag{B7}$$

which can be used instead of L as a propagator for the coupled equations in the nondiabatic representation. The same suggestion, though preceded by a different

[2] This is the point where we differentiate the propagators in nondiabatic representation from the propagators in diabatic representations.

argumentation and concerning the log-derivative matrix (i.e., the block $L^{(4)}$) only has been made recently by Macek [22]. Actually, the matrix $\tilde{L}$ had been already exploited in the derivation of the generalized log-derivative method [12].

In the paper [12] we considered the matrix $\tilde{L}$ as a mixture of the $\mathscr{L}$-type propagators in the nondiabatic and in two different diabatic representations,

$$\tilde{L}(u', u'') = \begin{pmatrix} L_{u'}^{(1)}(u', u'') & L^{(2)}(u', u'') \\ L^{(3)}(u', u'') & L_{u''}^{(4)}(u', u'') \end{pmatrix}, \tag{B8}$$

where $L_{\bar{u}}(u', u'') = \hat{L}[I^- \Omega_{\bar{u}}(u'', u')]$ for $\bar{u} = u', u''$. $\Omega_{\bar{u}}$ is the standard propagator which satisfies the equations

$$\frac{d}{du}\Omega_{\bar{u}}(u, u') = \begin{pmatrix} 0 & 1 \\ -b_{\bar{u}}(u) & 0 \end{pmatrix}\Omega_{\bar{u}}(u, u'), \qquad \Omega_{\bar{u}}(u', u') = 1,$$

with the matrix $b_{\bar{u}}$ related to the matrix b through the relations (17a), (16).

Here we complete the $\mathscr{L}$-matrix formalism with the relation

$$\tilde{L}(u', u'') = \hat{L}[I^- \tilde{\Omega}(u'', u')], \tag{B9}$$

and we state that the matrix $\tilde{\Omega}$ satisfies the following equations:

$$\frac{d}{du}\tilde{\Omega}(u, u') = \begin{pmatrix} -\frac{1}{2}A(u) & 1 \\ -b(u) & -\frac{1}{2}A(u) \end{pmatrix}\tilde{\Omega}(u, u'), \qquad \tilde{\Omega}(u', u') = 1. \tag{B10}$$

$\tilde{\Omega}$ represents simply another choice of a standard propagator for Eq. (B1). Thus, according to the assumed definitions the matrix $\tilde{L}$ can be viewed in the same way as the matrix L, i.e., as an $\mathscr{L}$-type propagator in the nondiabatic representation. Clearly, the difference in the symmetry properties between the matrices $\tilde{L}$ and L should be visible at the level of the corresponding standard propagators. Indeed, the relation (B5) for the matrix Ω rewritten in terms of the matrix $\tilde{\Omega}$ takes the form of the following unitarity (J_--unitarity) condition:

$$\tilde{\Omega}^T(u'', u')\, J_-\, \tilde{\Omega}(u'', u') = J_-, \qquad \text{where} \quad J_- = \begin{pmatrix} 0 & 1 \\ -1 & 0 \end{pmatrix}. \tag{B11}$$

The same condition satisfies the matrix $\Omega_{\bar{u}}$ and it is a matter of some algebraic manipulations to check that the J_--unitarity of the standard propagators really guarantees symmetry of the corresponding $\mathscr{L}$ matrices.

To give evidence of consistency of the formula (B9) with the previous formula (B8) we show that both formulas lead to the same differential equations for the matrix $\tilde{L}$. To this end we exploit the differential equations derived elsewhere [11, 23] in the form valid generally for any propagator $l(u', u'')$, $l = \begin{pmatrix} l_1 & l_2 \\ l_3 & l_4 \end{pmatrix}$, related to a standard propagator $\omega(u'', u')$ trough the operation $\hat{L}$; $l(u', u'') = \hat{L}[I^- \omega(u'', u')]$.

These equations involve the coupling matrix a, $a = \left(\begin{smallmatrix} a_1 & a_2 \\ a_3 & a_4 \end{smallmatrix}\right)$ occurring in the initial value problem for ω,

$$\frac{d}{du}\,\omega(u, u') = a(u)\,\omega(u, u'), \qquad \omega(u', u') = 1,$$

and read

$$\frac{d}{du}\,l_1(u', u) = -l_2(u', u)\,a_2 l_3(u', u),$$

$$\frac{d}{du}\,l_2(u', u) = l_2(u', u)[-a_1 + a_2 l_4(u', u)],$$

$$\frac{d}{du}\,l_3(u', u) = [a_4 + l_4(u', u)\,a_2]\,l_3(u', u),$$

$$\frac{d}{du}\,l_4(u', u) = -a_3 + a_1 l_4(u', u) - l_4(u', u)\,a_1 + l_4(u', u)\,a_2 l_4(u', u).$$

One set of equations for the matrix $\tilde{L}$ we get by the simple substitution:

$$a = \begin{pmatrix} -\frac{1}{2}A & 1 \\ -b & -\frac{1}{2}A \end{pmatrix}.$$

To derive the set originating in the formula (B8) we have, of course, substitute different a's for different blocks of $\tilde{L}$, i.e., $\left(\begin{smallmatrix} 0 & 1 \\ -b_{\bar{u}} & 0 \end{smallmatrix}\right)$ with $\bar{u} = u'$, u or $\left(\begin{smallmatrix} 0 & 1 \\ -B & -A \end{smallmatrix}\right)$. Moreover, to get the correct form of $(d/du)\,L_u^{(4)}(u', u)$ we have to proceed through the intermediate step of transforming $L_u^{(4)}(u', u)$ to a different diabatic representation, e.g., $L_u^{(4)}(u', u) = t(u; u')\,L_u^{(4)}(u', u)\,t^T(u; u')$. To see the identity of both systems we have to refer also to the more general form of Eq. (B8) (given in [12]),

$$\tilde{L}(u', u'') = \begin{pmatrix} t(u'; \bar{u}) & 0 \\ 0 & t(u''; \bar{u}) \end{pmatrix} L_{\bar{u}}(u', u'') \begin{pmatrix} t^T(u'; \bar{u}) & 0 \\ 0 & t^T(u''; \bar{u}) \end{pmatrix}. \tag{B12}$$

ACKNOWLEDGMENTS

The author thanks Professor Don Secrest for his interest in this work and Professor L. Wolniewicz for critical reading of the manuscript. This work was supported by the Polish Ministry of Higher Education and Science within project MR.I.5 and a grant from the U.S. National Science Foundation.

REFERENCES

1. D. SECREST, in *A Guide for the Experimentalists*, edited by R. B. Bernstein (Plenum, New York, 1979), p. 265.
2. G. A. PARKER, J. G. SCHMALZ, AND J. C. LIGHT, *J. Chem. Phys.* **73**, 1757 (1980).

3. G. A. PARKER, J. V. LILL, AND J. C. LIGHT, National Resource for Computation in Chemistry Software Catalog, Program No. KQ04 VIVAS, 1980; G. A. Parker, J. C. Light, and B. R. Johnson, *Chem. Phys. Lett.* **73**, 572 (1980).
4. L. D. THOMAS, M. H. ALEXANDER, B. R. JOHNSON, W. A. LESTER, JR., J. C. LIGHT, K. D. MCLENITHAN, G. A. PARKER, M. J. REDMON, T. G. SCHMALZ, D. SECREST, AND R. B. WALKER, *J. Comput. Phys.* **41**, 407 (1981).
5. R. B. WALKER, Quantum Chemistry Program Exchange, Program No. 352, 1978.
6. J. C. LIGHT AND R. B. WALKER, *J. Chem. Phys.* **65**, 4272 (1976).
7. E. B. STECHEL, R. B. WALKER, AND J. C. LIGHT, *J. Chem. Phys.* **69**, 3518 (1978).
8. D. J. ZVIJAC AND J. C. LIGHT, *Chem. Phys.* **12**, 237 (1976).
9. B. R. JOHNSON, *J. Comput. Phys.* **13**, 445 (1973).
10. B. R. JOHNSON, "Proceedings of the NRCC Workshop on Algorithms and Computer Codes in Atomic and Molecular Quantum Scattering Theory," Lawrence Berkeley Report LBL-9501, 1979.
11. F. MRUGALA AND D. SECREST, *J. Chem. Phys.* **78**, 5954 (1983).
12. F. MRUGALA AND D. SECREST, *J. Chem. Phys.* **79**, 5960 (1983).
13. R. B. WALKER, J. C. LIGHT, AND A. ALTENBERGER-SICZEK, *J. Chem. Phys.* **64**, 1166 (1976).
14. R. D. MARCUS, *J. Chem. Phys.* **45**, 4493, 4500 (1966); **49**, 2610 (1968).
15. M. V. BASILEVSKY, *J. Mol. Struct.* **103**, 139 (1983).
16. F. MRUGALA, *J. Comput. Phys.* **58**, 113 (1985).
17. R. N. PORTER AND M. KARPLUS, *J. Chem. Phys.* **40**, 1105 (1964).
18. J. T. MUCKERMAN, *J. Chem. Phys.* **56**, 2997 (1972).
19. N. A. MULLANEY AND D. G. TRUHLAR, *Chem. Phys.* **39**, 91 (1979).
20. J. C. LIGHT AND R. B. WALKER, *J. Chem. Phys.* **63**, 1598 (1976).
21. B. C. GARRETT AND D. G. TRUHLAR, *Theoretical Chemistry: Advances and Perspectives*, Vol. 6A (Academic Press, New York, 1981), p. 215.
22. J. MACEK, *Phys. Rev. A* **30**, 1275 (1984).
23. F. MRUGALA, *Chem. Phys.* **49**, 241 (1980).
24. A. KUPPERMANN, J. A. KAYE, J. P. DWYER, *Chem. Phys. Lett.* **74**, 257 (1980); G. HAUKE, J. MANZ, AND J. RÖMELT, *J. Chem. Phys.* **73**, 5040 (1980).